DE GRUYTER

Chemical Papers 70 (12) 1632–1641 (2016)
DOI: 10.1515/chempap-2016-0100

ORIGINAL PAPER

Co-precipitation behaviour of titanium-containing silicate solution

Hui-Hong Lü*, Min-Zhi Wu, Zheng-Li Zhang, Xing-Rong Wu, Liao-Sha Li, Zhi-Fang Gao

Key Laboratory of Metallurgical Emission Reduction & Resources Recycling, Ministry of Education, Anhui University of Technology, Hudong Road 59, Ma'anshan, 243002 Anhui, China

Received 7 January 2016; Revised 20 May 2016; Accepted 20 May 2016

The co-precipitation behaviour of a simulated $Al_2(SO_4)_3$–$TiOSO_4$–Na_2SiO_3 solution that imitated the lixivium of Ti-bearing blast furnace slag (Ti-slag) leached by sulphuric acid was investigated in this study. Various chemical analyses were employed to study the selective precipitation of multiple target components. Based on the high-added-value applications of Ti-slag, a new method was developed to prepare aluminium titanate composites from titanium-containing silicates. The findings demonstrate that the onsets of Ti and Al precipitation occur at pH values of 3.5 and 5.0, respectively, followed by Si precipitation. The particle sizes of the co-precipitates were greatly influenced by the precipitants, pH and the initial Al/Ti mole ratio. The results also show that the precipitation ratio of Ti, Al and Si generally increases with the pH and temperature, regardless of the Al/Ti mole ratio. The Si-O-Al, Ti-O-Al, and Ti-O-Si bonds that were formed were dependent on the pH and the initial Al/Ti mole ratio. There was a synthesis path for β-Al_2TiO_5 (AT) from the solid-state reaction between rutile and α-Al_2O_3 at 1362.5 °C. The AT composites were successfully prepared by sintering the co-precipitates at 1450 °C, which exhibited good thermal stability as estimated by the XRD measurements of the sample annealed at 1200 °C for 4 hours.

Keywords: co-precipitation behaviour, resources, aluminium titanate composites, titanium containing silicates, Ti-slag

Introduction

China holds most of the global titanium resources, approximately 90 % of which are located in Panzhihua. Nearly all of this titanium is transformed into slag consisting of 22 % TiO_2 after the blast furnace iron-making process. There are currently more than 70 million tonnes of Ti-slag, increasing by 3 million tonnes per year, in the Panzhihua area (Chen et al., 2013).

Ti-slag represents a valuable resource, and several studies have focused on the reuse of Ti-slag. These include using carbide–chloride to generate $TiCl_4$, leaching Ti with acid or molten salt to create raw materials to prepare TiO_2 after removing vanadium, or producing a Si–Ti alloy by the direct electrolytic method. However, these Ti-slag treatment approaches focus on the recovery of only one chemical component. Accordingly, the present study develops a new method to reuse several components of Ti-slag in a single process. To this end, multi-doped $LiFePO_4$ was prepared from steel slag (Wu et al., 2010) and perovskite $CaTiO_3$ was directly extracted from Ti-slag (Lü et al., 2013). Hydrometallurgy is generally used to leach low-grade valuable single components in high-silicon metallurgical slag; however, the concomitant silicic acid products polymerise and gelatinise during the subsequent precipitation of the valuable components, leading to difficulties in product purification.

Due to the complexity of the components and the presence of acidic, basic and amphoteric elements in silicon metallurgical slag (such as Ti-slag), it is difficult to precipitate multi-target components, resulting in few value-added uses for the slag. Hence, it

*Corresponding author, e-mail: lv_huihong@163.com

was necessary to resolve the key scientific problems of controlling the combined precipitation of the target components and the particle growth mechanism in the titanium-containing silicate in the basic co-precipitation process. To solve the above problems, aluminium titanate and cordierite composites were successfully prepared from Ti-slag and blast furnace slag, respectively, rather than recovering single-target components (Wu et al., 2013a).

This study yields evidence for the combined precipitation of target components in titanium-containing silicates and suggests promising high-value uses for Ti-slag. For example, an aluminium titanate ceramic material was successfully prepared from Ti-slag rather than recycling the single components (Wu et al., 2013b).

Aluminium titanate (AT) is a promising material due to its excellent properties, including low thermal conductivity, excellent thermal shock resistance and high thermal expansion anisotropy. The traditional method of preparing AT is based on a solid-state reaction between stoichiometric mixtures of titanium(IV) oxide and aluminium(III) oxide above 1300 ℃ (Sobhani et al., 2014). However, the phase composition is extremely heterogeneous due to significant quantities of unreacted TiO_2 and Al_2O_3. Furthermore, the AT formed from TiO_2 and Al_2O_3 decomposes to rutile and alumina at temperatures of 800–1300 ℃ (Xie et al., 2010). Additives such as Al_2O_3, SiO_2 and mullite have been considered for improving the thermal stability of the process (Huang et al., 1998; Oikonomou et al., 2007; Xie et al., 2010). The conversion of industrial wastes into valuable products has several advantages over the traditional chemical preparation of materials in terms of the conservation of resources, the environment and energy (Kim et al., 2011). As a convenient and cost-effective method for synthesising precursors from inorganic salt solutions, co-precipitation has attracted widespread attention. Co-precipitation is also an important metallurgical method for recovering valuable elements in metallurgical slags. Despite the importance of this issue and the abundance of raw materials for this purpose, few studies have provided detailed chemical, structural and material investigations regarding the co-precipitation process for solutions of titanium-containing silicates (Kimura et al., 2006; Kurc, 2014).

The co-precipitation behaviour of a simulated $Al_2(SO_4)_3$–$TiOSO_4$–Na_2SiO_3 solution leached from Ti-slag by sulphuric acid was examined in this study. The study sought to clarify the selective precipitation of multiple-target components and to design a new method for preparing AT composites from the co-precipitates.

Experimental

The following chemicals were purchased from the indicated suppliers and used without further purification: $Al_2(SO_4)_3 \cdot 18H_2O$, $Na_2SiO_3 \cdot 9H_2O$, NH_4OH, NaOH and absolute ethanol (Sinopharm Chemical Reagent, Shanghai, China, AR), sulphuric acid (Oriental Chemical Reagent Company, Liyang, China, 98 mass %) and $TiOSO_4$ (Aladdin Industrial Corporation, Shanghai, China, 93 mass %). The solutions were adjusted to the required concentrations using de-ionised water.

The co-precipitation was carried out in a 2-L jacketed glass reactor. First, 26.65 g of $Al_2(SO_4)_3 \cdot 18H_2O$ and 2.84 g of $Na_2SiO_3 \cdot 9H_2O$ were dissolved in 200 mL of de-ionised water. Then, 3.44 g of $TiOSO_4$ was dissolved in 100 mL of 2 mol L^{-1} sulphuric acid solution. Next, the prepared $Al_2(SO_4)_3 \cdot 18H_2O$, $TiOSO_4$ and $Na_2SiO_3 \cdot 9H_2O$ solutions were mixed in a 1-L volumetric flask to volume with a 2 mol L^{-1}sulphuric acid solution (Al-Ti-Si solution). Thus, a Ti-Al-Si ternary solution with: $C(Al^{3+}) = 40.0$ mM, $C(Ti^{4+}) = 20.0$ mM and $C(Si^{4+}) = 10.0$ mM was obtained. Bases (NH_4OH or NaOH solutions) were added quickly (approximately 5 mL min^{-1}), and each titration was completed within approximately 60 min. The solution containing suspended particles was then allowed to equilibrate for an additional 2 hours. Subsequently, the solution containing co-precipitates were washed to remove excess salts by repeated centrifuging and re-suspending in de-ionised water. The co-precipitates were finally dried in an oven at 115 ℃ for 6 hours and were then used for the following measurements.

The final AT composites were obtained by calcinating the co-precipitates at 1350 ℃ and 1450 ℃ for 3 hours at each temperature, using a heating rate of 5 ℃ min^{-1} in a high temperature furnace designed for the purpose (Li et al., 2010) under an air atmosphere.

The chemical composition of the precipitates was determined using an ICPS-7510 ICP-OES instrument (Shimadzu, Kyoto, Japan). The FTIR spectra of the samples were obtained with a 6700 system (Thermo Nicolet, Waltham, MA, USA) using the KBr disk method. TG-DSC measurements were carried out on a STA449 F3 simultaneous thermal analyser (Netzsch, Selb, Germany) from ambient temperature to 1400 ℃ under an N_2 atmosphere at a 5 ℃ min^{-1} heating rate. The phase analyses of the precipitates and the AT composites were measured using a D8 Advance X-ray diffractometer (Bruker AXS, Karlsruhe, Germany) with a CuK_α radiation source ($\lambda = 1.5406$ Å) of 40 kV, 30 mA and a scanning speed of 3° min^{-1} over a 2θ range of 10–80°. The contents of the main crystalline phases of the AT composites were obtained through a Rietveld quantitative analysis with Fullprof software. The particle sizes were measured using a Rise-2006 granulometer (Runzhi, Jinan, China). A pHS-2CW pH meter (Bante, Beijing, China) was used to monitor the changes in pH of the $Al_2(SO_4)_3$–$TiOSO_4$–Na_2SiO_3 solution upon titration with the precipitants. The morphologies of the co-precipitates

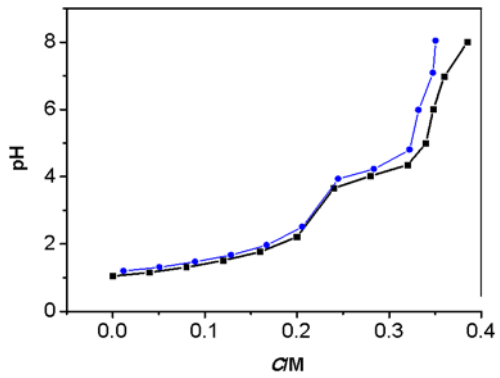

Fig. 1. Change in pH of $Al_2(SO_4)_3$–$TiOSO_4$–Na_2SiO_3 solution upon titration by NH_4OH (■) and NaOH (●) precipitants under initial conditions $C_{Ti} = 1.0 \times 10^{-2}$ M and Al : Tia : Si = 2 : 1 : 0.5 at reaction temperature of 25.0 °C.

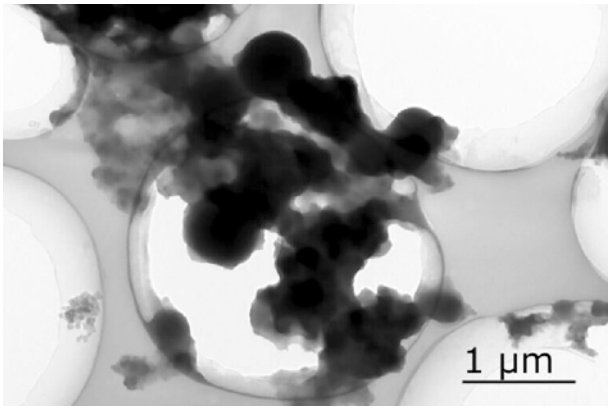

Fig. 2. TEM morphologies of onset precipitates titrated by NH_4OH precipitants under initial conditions $C_{Ti} = 1.0 \times 10^{-2}$ M and Al : Ti : Si = 2 : 1 : 0.5 at reaction temperature of 25.0 °C and pH 3.5.

and AT composites were characterised using an S4800 scanning electron microscope (SEM, Hitachi, Osaka, Japan). The morphologies of the onset precipitates at pH 3.5 were recorded by a JEM2100 transmission electron microscope (TEM, JEOL, Tokyo, Japan).

Results and discussion

The formation of mixed Ti-Al-Si oxyhydroxy co-precipitates from $Al_2(SO_4)_3$–$TiOSO_4$–Na_2SiO_3 dilute sulfuric acid solutions titrated by NH_4OH and NaOH was recorded as potentiometric (pH) titration curves (Fig. 1). Two distinct pH plateaux were observed, which corresponded to the neutralisation reaction between OH^- and H^+ in the Al-Ti-Si solution below pH 1.9 and the onset of Ti precipitation at pH 3.5, followed by Al precipitation at pH 5. The Al/Ti mole ratio in the co-precipitate formed at pH 5 was 2.2 : 1.0, which was larger than the ratio of 1.0 : 4.8 in the precipitate formed at pH 3.5.

The Ti-Al-Si aqueous solutions used in this study were colloidal and contained complex species. However, the co-precipitation was due to the low solubility of $Al(OH)_3$, $TiO(OH)_2$ and their complex silicates.

The TEM and SEM morphologies of the co-precipitates of Ti-Al-Si in Fig. 2 and Fig. 3a, respectively, showed that most of the particles were fine and homogeneous, with a particle size of approximately 3 μm. The average particle size of the AT composites sintered at 1450 °C for 3 hours (Fig. 3c) was approximately 200 nm.

Fig. 4 illustrates the relationship between the average particle size and the co-precipitation conditions. Fig. 4a indicates that the particle size of the co-precipitates increased markedly with the reaction temperature. The effect of the reaction temperature on the co-precipitate size can be ascribed to the effect of the reaction temperature on the precipitation kinetics, including the nucleation and growth rates. At high temperatures, the growth rate is higher than the nucleation rate, so the particles become larger (Lee et al., 2009). According to the electric double layer and DLVO theories, the metallic cations (Na^+ in NaOH) increased the electrostatic interaction of the particles. Hence, the micrometre-sized particles formed by NaOH as a co-precipitant are generally larger than those formed by NH_4OH as a co-precipitant while varying each of the three conditions, temperature, pH and Al/Ti mole ratio, as shown in Figs. 4a–4c, respectively.

Fig. 4b shows that the particle sizes of co-precipitates at pH 7 were relatively small. Almost amorphous $Al(OH)_3$ was formed at pH 5–6, and some portion of the bayerite (α-$Al(OH)_3$) phase co-precipitated at pH 8. The differences in particle size in relation to the precipitation pH of the aluminium hydroxides was also observed by Du et al. (2009). Furthermore, the isoelectric points of SiO_2 (Richmond et al., 1998), $Al(OH)_3$ (El-Masry et al., 2004) and TiO_2 hydrosol (Wellia et al., 2011) (i.e., $TiO(OH)_2$) were below the pH ranges of 4, 7.5–8.5 and 4.5–6.8, respectively. At pH values lower than the isoelectric points, the positively charged Al-Ti-Si hydroxides are attracted to the negatively charged particles. The increase in the negative charge on the surface of the colloid particles results in a strong surface electrostatic force which obstructs the agglomeration of hydroxide particles and produces small floccules. The OH^- ions provided by the NH_4OH solution (at pH 7) dissolved the $Al(OH)_3$ to form AlO^{2-} ions (Pourbaix et al., 1974), and higher concentrations (at pH 8) resulted in heterogeneous co-precipitation with median particle size changes, as shown in Fig. 4b.

Fig. 4c shows that the smallest co-precipitate formed at the stoichiometric ratio of Al/Ti for Al_2TiO_5. Under acidic conditions, hydration of the OH groups on the surface of the silica particles can lead to particle agglomeration. In addition, $Al(OH)_3$ reacting with an acid results in the formation of Al^{3+}

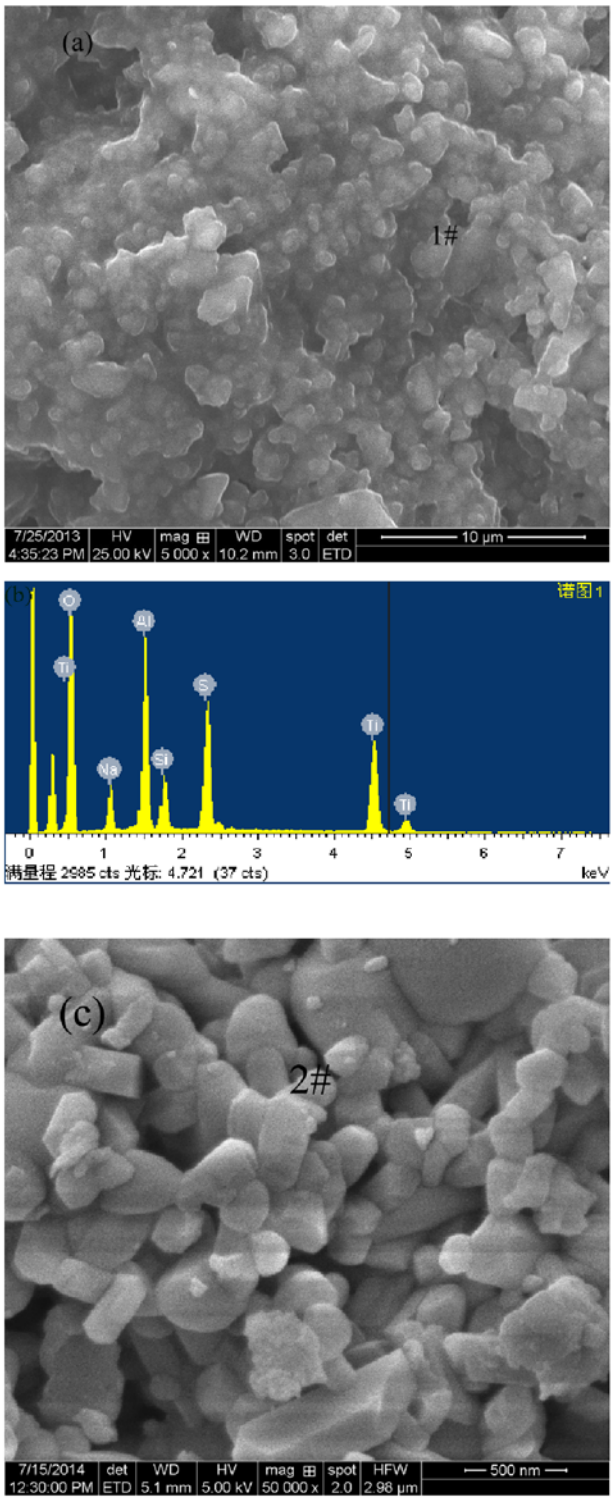

Fig. 3. SEM morphologies of precipitates titrated by NH_4OH precipitants under initial conditions $C_{Ti} = 1.0 \times 10^{-2}$ M and Al : Ti : Si = 2 : 1 : 0.5 at reaction temperature of 25.0 °C and pH 5 (a), EDS of spot (1#) in Fig. 3a (b) and SEM morphologies of sample A sintered at 1450 °C for 3 hours (c).

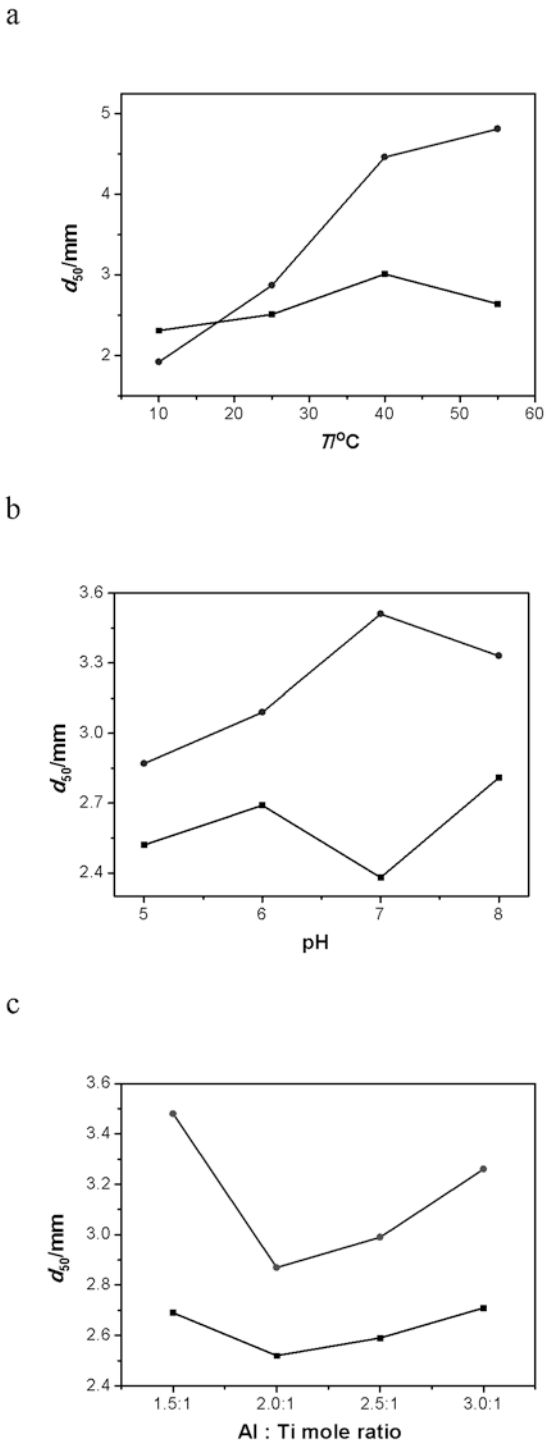

Fig. 4. Median particle size (d_{50}) of precipitates titrated by NH_4OH (■) and NaOH (●) with initial $C_{Ti} = 1.0 \times 10^{-2}$ M $Al_2(SO_4)_3$–$TiOSO_4$–Na_2SiO_3 solution which was dependent on the co-precipitation conditions: reaction temperature (a), co-precipitation pH (b) and Al/Ti mole ratio (c).

ions, which act as counterions adsorbed on the surface of the silica particles. This proximity of the Al^{3+} and SiO_2 particles causes the gel to become more homogeneous. Under acidic conditions, the increasing amount of OH^- leads to condensation reactions between the $Al(OH)_3$ particles, $Al(OH)_3$ and SiO_2 particles, result-

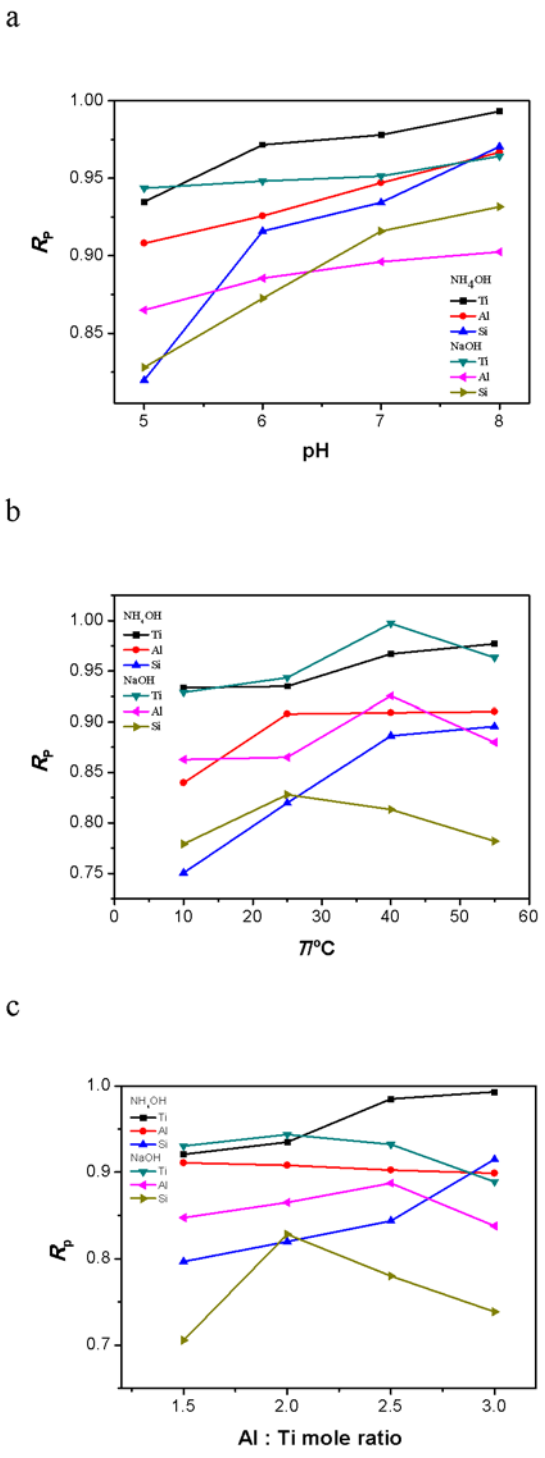

Fig. 5. Precipitation ratio of $Al_2(SO_4)_3$–$TiOSO_4$–Na_2SiO_3 solution with initial $C_{Ti} = 1.0 \times 10^{-2}$ M titrated by NH_4OH, as dependent on co-precipitation conditions: reaction temperature (a), co-precipitation pH (b) and Al/Ti mole ratio (c).

ing in segregations of the alumina and silica (Huang et al., 1997).

Fig. 5 displays the relationship between the precipitation ratio of Ti, Al and Si (R_p), in which R_p is the mole ratio of the relative element in the co-precipitates and the initial element in the stock solution analysed by ICP under various co-precipitation conditions. Fig. 5a shows that R_p generally increased with increasing pH. The pH in the solution dictates the extent to which the water molecules are replaced, depending on the availability of OH^-. Thus, various aluminium hydroxide mononuclear species can be formed.

Because it has zero charge and is capable of condensing to form the solid phase, $Al(OH)_3$ is formed at sufficiently high concentrations of OH^-. The dimeric, trimeric and polynuclear hydrolysis products of Al^{3+} can be formed in high concentrations of OH^-; however, these products are often ignored, especially in dilute solutions (Duan & Gregory, 2003). Accordingly, combined with the comprehensive effect of the isoelectric points of SiO_2, $Al(OH)_3$ and $TiO(OH)_2$, R_p increases with an increase in pH.

However, silica gel was dominant in the silicic-acid-containing solution at the pH studied (Li & Lu, 2011). Heterogeneous condensation occurred for the aluminium, silicic and titanium hydroxides to form aluminium–silicon, titanium–silicon and aluminium–titanium polymers. This was further confirmed by FTIR measurements.

Fig. 5b shows that the R_p values of Al, Ti and Si were influenced by the co-precipitation temperature. A high temperature often promotes agglomeration and the growth of aluminium, silicic and titanium hydroxide colloids. Hence, the precipitation ratio increased with the reaction temperature. Fig. 5c indicates that the initial Al/Ti mole ratio had no apparent effect on R_p.

FTIR spectroscopy provides important information on the chemical composition and structure of amorphous materials. Figs. 6a–6c show the ambient temperature FTIR transmittance spectra of the co-precipitates prepared under various pHs, reaction temperatures and Al/Ti mole ratios measured in the 400–4000 cm^{-1} regions, respectively. The broad bands at ≈ 3400 cm^{-1} and ≈ 1636 cm^{-1} may be due to the O—H stretching vibration of the $TiO(OH)_2$, $Al(OH)_3$, $Si(OH)_4$, their complex oxyhydroxy co-precipitates and the residual water. A slight shift in the higher wavenumbers in the O—H stretching vibration band at ≈ 3400 cm^{-1} indicates bond weakening because of the increasing Si—O—Al, Ti—O—Al and Ti—O—Si bond formation with the increasing reaction temperature, co-precipitation pH and Al/Ti mole ratio. The band at 1135 cm^{-1} is related to the stretching vibration of Si—O (Schneider & Komarneni, 2005; Li & Lu, 2011) or the bending vibration of Ti—O—Al (Di Valentin et al., 2007). The bands at 981 cm^{-1}, attributed to the bending vibration of Si—O—Al (Aravind et al., 2006) or the stretching vibration of Ti—O—Si (Matsuda et al., 2006), are enhanced with the co-precipitation pH increase, accompanied by the gradual disappearance of the band at 1135 cm^{-1}. The

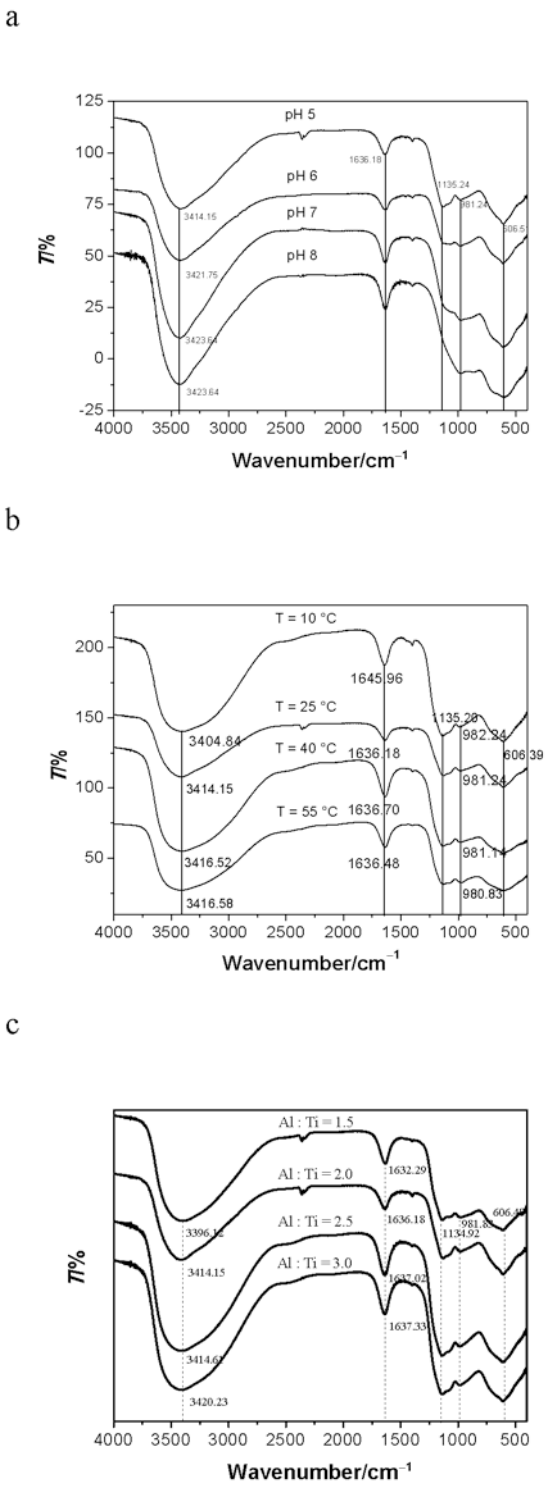

Fig. 6. FTIRspectra of co-precipitates prepared by NH_4OH under various co-precipitation conditions: co-precipitation pH (a), reaction temperature (b) and Al/Ti mole ratio (c).

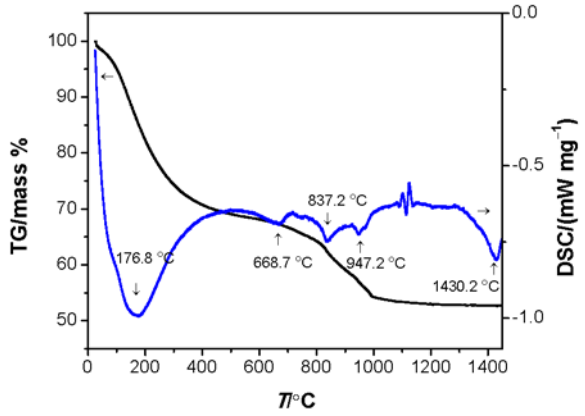

Fig. 7. TG-DSC (in an air atmosphere) curves of AT precursor co-precipitated in $Al_2(SO_4)_3$–$TiOSO_4$–Na_2SiO_3 solution and titrated by NH_4OH under initial conditions of $C_{Ti} = 1.0 \times 10^{-2}$ M and Al : Ti : Si = 2 : 1 : 0.5 at 25.0 °C.

increase in the Si—O—Al and Ti—O—Si bonds in the samples is further confirmed by the increase in Al and Ti in the co-precipitates with a pH increase. This indicates that Al and Ti existed as segregated amorphous SiO_2 particles and that some fraction of their bonding was Si—O—Si. As expected, the intense band at 606 $cm^{-1}$was due to the bending vibration of Al—OH (Farmer, 1974), which increased with the Al/Ti mole ratio. The variation in the characteristic peaks, such as for M—OH (M = Ti, Al and Si), Ti—O—Al, Si—O—Al and Ti—O—Si, is evidence of the complex co-precipitation, including homogeneous and heterogeneous condensation reactions between $Al(OH)_3$, $TiO(OH)_2$ and $Si(OH)_4$ colloidal particles.

Fig. 7 shows that the TG-DSC analyses for the AT composite precursors exhibited a significant loss of ignition (LOI) from ambient temperature to 320 ℃. The endothermic peak appearing at 176.8 ℃ was associated with the vaporisation of the physically absorbed water and the removal of the surface and structural hydroxyls, respectively. From 320 ℃ to 1000 ℃, the mass loss may have been due to the de-hydroxylation of the $TiO(OH)_2$–$Al(OH)_3$–$Si(OH)_4$ inorganic moieties and the decomposition of ammonia sulphates. The endothermic peak at 668.2 ℃ can be attributed to the conversion of anatase to rutile, in which the addition of Al_2O_3 (Jung et al., 2008) and SiO_2 (Periyat et al., 2008) to the TiO_2 prevented the phase transformation. There was a 10 % mass loss from approximately 800 ℃ to 1000 ℃ resulting in endothermic peaks at 837.3 ℃ and 947.2 ℃ due to the thermal decomposition of the metallic sulphates. Between 1000 ℃ and 1400 ℃, the smooth changes in mass indicate that all of the sulphates decomposed. The exothermic peak at approximately 1100 ℃ may be attributed to the formation of metastable mullites (Chakravorty & Ghosh, 1988). The endothermic peak at 1430.2 ℃ can be clearly assigned as the synthesis of β-Al_2TiO_5 from rutile TiO_2 and α-Al_2O_3.

The formation of mullite and AT at low temperatures occurred for the following reasons: the EDS map of the onset precipitates at pH 3.5 shows a Ti : Al : Si

mole ratio of 4.8 : 1.0 : 1.1. Together with the FTIR results, this ratio indicates that a weak van der Waals interaction formed between the titanium-silica core and alumina layer (El-Masry et al., 2004) in the co-precipitation stage. However, during the dehydroxylation of the $TiO(OH)_2$–$Al(OH)_3$–$Si(OH)_4$ process (below 720 ℃), the Ti—O—Al and Si—O—Al linkages were enhanced. Thus, the mullite and the AT crystallisation evolved more easily.

Okada and Otsuka (1986) noted that M_1—O—M_2 linkages (M_1 = Si, M_2 = Al in the case of mullite) are an important factor for determining the crystallisation phase. The exothermic peak at 1269.1 ℃ indicates the formation of α-Al_2O_3 from γ-$A1_2O_3$ at a transformation temperature that is approximately 95 ℃ higher than that from a previous study (Liu et al., 2013). The thermal stability of γ-Al_2O_3 was found to improve significantly in the presence of some additives, such as SiO_2 (Belver et al., 2002; Liu et al., 2008) and TiO_2 (Zhou et al., 2007), hence the transformation of γ-Al_2O_3 into α-$A1_2O_3$ was significantly retarded. A small endothermic peak at 1362.5 ℃ was attributed to the solid-state reaction of β-Al_2TiO_5 between rutile TiO_2 and α-Al_2O_3.

Fig. 8a displays the XRD pattern of the co-precipitate prepared under the conditions of initial $C_{Ti} = 1.0 \times 10^{-2}$ M and Al : Ti : Si = 2 : 1 : 0.5 at a reaction temperature of 25.0 ℃ after washing and drying. It is evident that the sample is in amorphous form, with a minor amount of anatase TiO_2. To determine whether the β-Al_2TiO_5 was synthesised at a lower temperature, a phase analysis of the co-precipitates sintered at 1350 ℃ was conducted. Fig. 6b clearly shows three crystalline phases: AT, rutile, and mullite. However, as shown in Table 1, when the co-precipitate was sintered at 1450 ℃, the metastable mullite vanished, but keatite and stishovite did not appear. The increase in β-Al_2TiO_5 and the de-

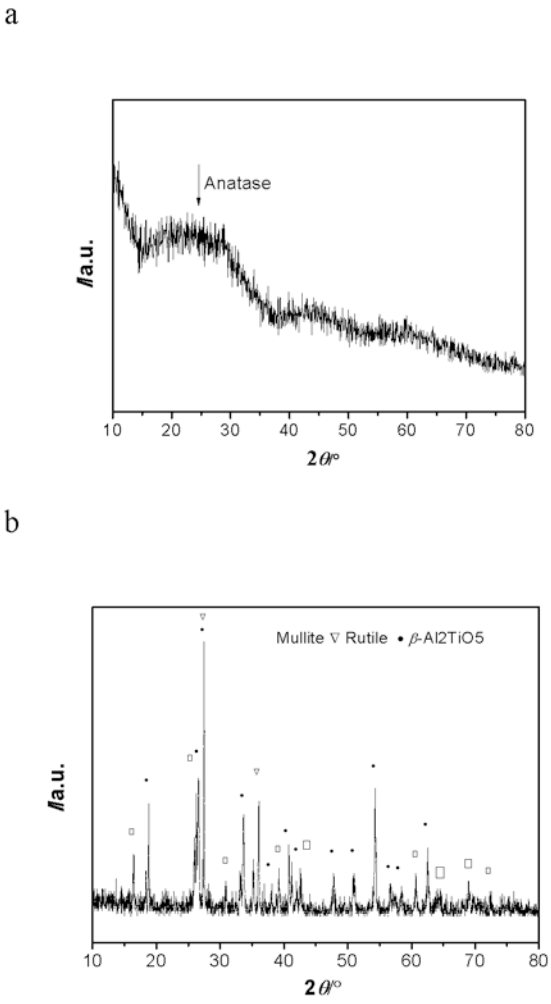

Fig. 8. XRD patterns of AT composite precursors co-precipitated in $Al_2(SO_4)_3$–$TiOSO_4$–Na_2SiO_3 solution titrated by NH_4OH under initial conditions of $C_{Ti} = 1.0 \times 10^{-2}$ M and Al : Ti : Si = 2 : 1 : 0.5 at 25.0 ℃ (a) and co-precipitates sintered at 1350 ℃ for 3 hours (b).

Table 1. Co-precipitation conditions, components of co-precipitates, sintering schedule (3 hours in all) and phase contents of AT composites

Co-precipitation conditions				Al : Ti : Si mole ratio in co-precipitates	Sintering T/℃	Phases[a] content of AT composites/mass %				
T/℃	C/M	Al : Ti : Si mole ratio	pH			β-AT	Rutile	Keatite	Stishovite	Mullite
10	1.0×10^{-2}	2 : 1 : 0.5	5	1.89 : 1 : 0.40	1450	89.9	3.5	6.0	0.6	0
25	1.0×10^{-2}	2 : 1 : 0.5	–	2.04 : 1 : 0.43	1450	84.5	1.5	9.2	4.8	0
					1350	34.6	16.5	0	0	48.9
40	1.0×10^{-2}	2 : 1 : 0.5	5	1.97 : 1 : 0.45	1450	91.2	1.1	7.5	0.2	0
55	1.0×10^{-2}	2 : 1 : 0.5	5	1.95 : 1 : 0.45	1450	90.7	0.5	7.0	1.9	0
25	1.0×10^{-2}	2 : 1 : 0.5	6	2.00 : 1 : 0.48	1450	91.7	0.7	6.4	1.2	0
25	1.0×10^{-2}	2 : 1 : 0.5	7	2.03 : 1 : 0.47	1450	92.4	0.6	6.5	0.5	0
25	1.0×10^{-2}	2 : 1 : 0.5	8	2.04 : 1 : 0.48	1450	92.2	1.3	6.2	0.4	0
25	1.0×10^{-2}	1.5 : 1 : 0.5	5	1.56 : 1 : 0.43	1450	78.1	13.3	8	0.6	0
25	1.0×10^{-2}	2.5 : 1 : 0.5	5	2.40 : 1 : 0.42	1450	73.0	0	11.3	1.5	14.2
25	1.0×10^{-2}	3 : 1 : 0.5	5	2.85 : 1 : 0.46	1450	65.9	0	3.9	0.6	29.6

a) The phases of β-AT, rutile, keatite, stishovite and mullite were attributed to the ref. codes of 01-070-1434, 01-072-1148, 01-076-0912, 01-080-0369 and 01-073-1389 in the Fullprof software, respectively.

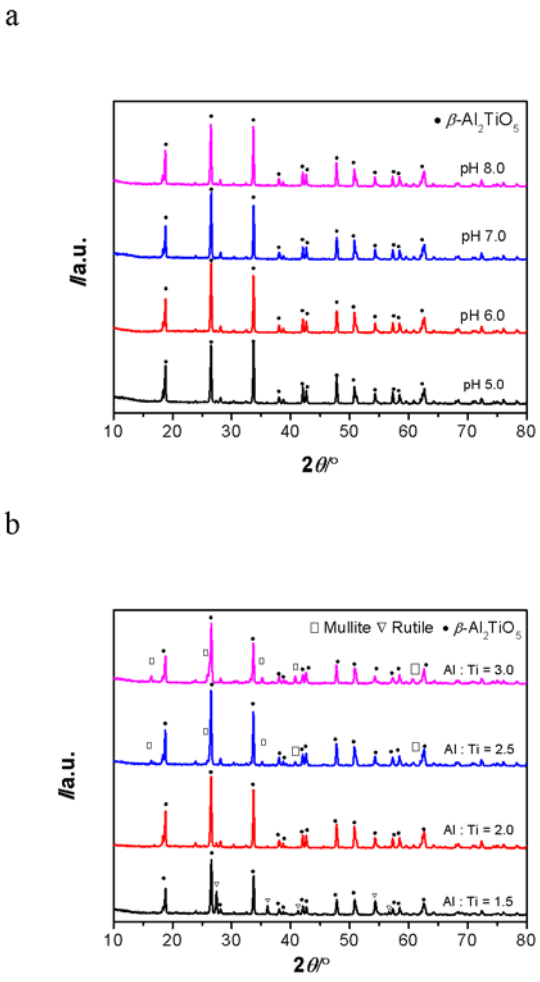

Fig. 9. XRD patterns of AT composites (sintered at 1450 ℃ for 3 h) co-precipitated under various conditions: co-precipitation pH (a) and Al/Ti mole ratio (b).

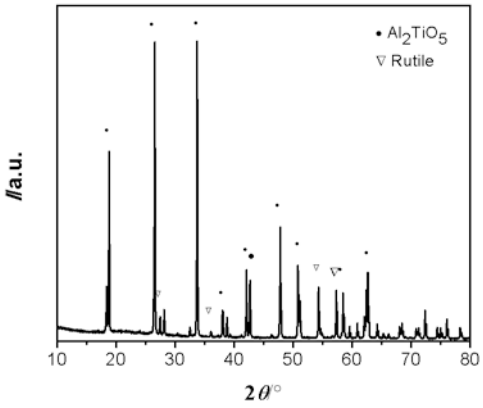

Fig. 10. XRD patterns of AT composites (sintered at 1450 ℃ for 3 h and annealed at 1200 ℃ for 4 hours) co-precipitated in $Al_2(SO_4)_3$–$TiOSO_4$–Na_2SiO_3 solution under initial conditions of C_{Ti} = 10.0 mM, Al : Ti : Si = 2 : 1 : 0.5 titrated by NH_4OH at 25.0 ℃.

crease in rutile were caused by the formation of β-AT from the solid-phase reaction between rutile TiO_2 and α-Al_2O_3, as discussed in the TG-DSC analyses for the AT composite precursors.

Fig. 9 shows the XRD pattern of the AT composites synthesised from co-precipitates under various conditions, the phase contents of which are also listed in Table 1. It is evident that β-Al_2TiO_5 appeared in the main crystal phase when the co-precipitates sintered at 1450 ℃ for 3 h, regardless of the pH, temperature or Al/Ti mole ratio. However, mullite formed in the samples that co-precipitated with an Al/Ti mole ratio that was higher than the stoichiometric ratio. In addition, mullite dominated in the sample sintered at 1350 ℃ for 3 h without the appearance of keatite and stishovite. This indicates that the metastable mullite was converted to keatite, stishovite and α-$A1_2O_3$ at temperatures above 1350 ℃. Hence, the specimen attained the second formation of β-Al_2TiO_5 by the solid-state reaction of rutile and α-$A1_2O_3$ at 1450 ℃.

The TG-DSC curves of the AT composites from precursors co-precipitated in the $Al_2(SO_4)_3$–$TiOSO_4$–Na_2SiO_3 solution under the initial conditions of C_{Ti} = 10.0 mM, Al : Ti : Si = 2 : 1 : 0.5 titrated by NH_4OH at 25.0 ℃ (a) and the mixture of rutile and α-Al_2O_3 with the stoichiometric ratio (b) sintered at 1450 ℃ for 3 h.

The XRD measurement was used to estimate the thermal stability of the AT. Fig. 10 presents the XRD pattern of the AT composites sintered at 1450 ℃ for 3 h and annealed at 1200 ℃ for 4 hours. α-$A1_2O_3$ cannot be detected, which indicates that the decomposition of β-Al_2TiO_5 could be ignored. The stability of β-Al_2TiO_5 may be attributed to the Si-doped AT composites precursor.

Conclusions

The co-precipitation behaviour of a simulated titanium-containing silicate solution leached from Ti-slag by sulphuric acid was investigated. Ti and Al were precipitated at 3.5 pH and 5.0 pH, respectively, followed by Si precipitation. The findings show that the precipitation ratios of Ti, Al and Si (R_p) generally increased with higher pH values and temperatures, regardless of the Al/Ti mole ratio. The co-precipitate particle size and the formation of AT were greatly influenced by the bonds of Si—O—Al, Ti—O—Al and Ti—O—Si. The bond formation of Si—O—Al, Ti—O—Al and Ti—O—Si was dependent on the experimental conditions. Accordingly, two synthesis paths for β-Al_2TiO_5 were identified, one from the rutile TiO_2 and amorphous Al_2O_3 at relatively low temperatures, and the other from the solid-state reaction between rutile TiO_2 and α-Al_2O_3 at higher temperatures. The results show that the AT composites synthesised by co-precipitates demonstrate good thermal stability from 800 ℃ to 1300 ℃ in comparison with the thermal decomposition and chemically syn-

thesised, self-recovered AT composites. These results resolve the key scientific problem of precipitation control for the target components in titanium-containing silicates in the basic co-precipitation process. These findings present a promising approach to preparing new, high-performance composite materials from Ti-slag.

Acknowledgements. This work was supported by grants from the National Natural Science Foundation of China (nos.51204004and51274006), University Science Research Project of Anhui Province (KJ2016A810), the Natural Science Foundation of China (U1660110) and Anhui Innovation Team Project of New Technology in Materialisation of Metallurgical Solid Wastes.

References

Aravind, P. R., Mukundan, P., Pillai, P. K., & Warrier, K. G. K. (2006). Mesoporous silica–alumina aerogels with high thermal pore stability through hybrid sol–gel route followed by subcritical drying. *Microporous and Mesoporous Materials*, *96*, 14–20. DOI: 10.1016/j.micromeso.2006.06.014.

Belver, C., Muńoz, M. A. B., & Vicente, M. A. (2002). Chemical activation of a kaolinite under acid and alkaline conditions. *Chemistry of Materials*, *14*, 2033–2043. DOI: 10.1021/cm0111736.

Chakravorty, A. K., & Ghosh, D. K. (1988). Synthesis and 980 °C phase development of some mullite gels. *Journal of the American Ceramic Society*, *71*, 978–987. DOI: 10.1111/j.1151-2916.1988.tb07568.x.

Chen, D. S., Zhao, L. S., Liu, Y. H., Qi, T., Wang, J. C., & Wang, L. N. (2013). A novel process for recovery of iron, titanium and vanadium from titanomagnetite concentrates: NaOH molten salt roasting and water leaching processes. *Journal of Hazardous Materials*, *244–245*, 588–595. DOI: 10.1016/j.jhazmat.2012.10.052.

Di Valentin, C., Finazzi, E., Pacchioni, G., Selloni, A., Livraghi, S., Paganini, M. C., & Giamello, E. (2007). N-doped TiO_2: Theory and experiment. *Chemical Physics*, *339*, 44–56. DOI: 10.1016/j.chemphys.2007.07.020.

Du, X. L., Wang, Y. Q., Su, X. H., & Li, J. G. (2009). Influences of pH value on the microstructure and phase transformation of aluminum hydroxide. *Powder Technology*, *192*, 40–46. DOI: 10.1016/j.powtec.2008.11.008.

Duan, J. M., & Gregory, J. (2003). Coagulation by hydrolysing metal salts. *Advances in Colloid and Interface Science*, *100–102*, 475–502. DOI: 10.1016/s0001-8686(02)00067-2.

El-Masry, M. H., Sadek, O. M., & Mekhemer, W. K. (2004). Purification of raw surface water using electro-coagulation method. *Water, Air & Soil Pollution*, *158*, 373–385. DOI: 10.1023/b:wate.0000044857.02199.45.

Farmer, V. C. (1974). *The infrared spectra of minerals*. London, UK: Mineralogical Society. DOI: 10.1180/mono-4.

Huang, Y. X, Senos, A. M. R., Rocha, J., & Baptista, J. L. (1997). Gel formation in mullite precursors obtained via tetraethylorthosilicate (TEOS) pre-hydrolysis. *Journal of Materials Science*, *32*, 105–110. DOI: 10.1023/a:1018575115770.

Huang, Y. X., Senos, A. M. R., & Baptista, J. L. (1998). Effect of excess SiO_2 on the reaction sintering of aluminium titanate-25 vol. % mullite composites. *Ceramics International*, *24*, 223–228. DOI: 10.1016/s0272-8842(97)00006-0.

Jung, Y. S., Kim, D. W., Kim, Y. S., Park, E. K., & Baeck, S. H. (2008). Synthesis of alumina–titania solid solution by sol–gel method. *Journal of Physics and Chemistry of Solids*, *69*, 1464–1467. DOI: 10.1016/j.jpcs.2007.10.037.

Kim, J. H., Kim, M. W., & Yu, J. S. (2011). Recycle of silicate waste into mesoporous materials. *Environmental Science & Technology*, *45*, 3695–3701. DOI: 10.1021/es103510r.

Kimura, T., Suzuki, M., Ikeda, T., Kato, K., Maeda, M., & Tomura, S. (2006). Silica-based mesoporous materials derived from Ti containing layered polysilicate kanemite. *Microporous and Mesoporous Materials*, *95*, 146–153. DOI: 10.1016/j.micromeso.2006.05.021.

Kurc, B. (2014). Gel electrolytes based on poly(acrylonitrile)/sulpholane with hybrid TiO_2/SiO_2 filler for advanced lithium polymer batteries. *Electrochimica Acta*, *125*, 415–420. DOI: 10.1016/j.electacta.2014.01.117.

Lee, S. O., Jung, K. H., Oh, C. J., Lee, Y. H., Tran, T., & Kim, M. J. (2009). Precipitation of fine aluminium hydroxide from Bayer liquors. *Hydrometallurgy*, *98*, 156–161. DOI: 10.1016/j.hydromet.2009.04.014.

Li, L. S., Liu, J. B., Wu, X. R., Ren, X., Bing, W. B., & Wu, L. S. (2010). Influence of Al_2O_3 on equilibrium sinter phase in N_2 atmosphere. *ISIJ International*, *50*, 327–329. DOI: 10.2355/isijinternational.50.327.

Li, L. S., & Lu, T. T. (2011). Condensation mechanism and influencing factor of stability of complicated silicic acid system. *AICHE Journal*, *57*, 1339–1343. DOI: 10.1002/aic.12374.

Liu, Q., Wang, A. Q., Wang, X. H., Gao, P., Wang, X. D., & Zhang, T. (2008). Synthesis, characterization and catalytic applications of mesoporous γ-alumina from boehmite sol. *Microporous and Mesoporous Materials*, *111*, 323–333. DOI: 10.1016/j.micromeso.2007.08.007.

Liu, P. C., Zhu, Y. Z., Ma, J. H., Yang, S. G., Gong, J. H., & Jian, X. (2013). Effect of boehmite sol on the crystallization behaviour and densification of mullite formed from a sol–gel precursor. *Progress in Natural Science: Materials International*, *23*, 145–151. DOI: 10.1016/j.pnsc.2013.02.004.

Lü, H. H., Li, N., Wu, X. R., Li, L. S., Gao, Z. F., & Shen, X. M. (2013). A novel conversion of Ti-bearing blast-furnace slag into water splitting photocatalyst with visible-light-response. *Metallurgical and Materials Transaction B*, *44*, 1317–1320. DOI: 10.1007/s11663-013-9973-y.

Matsuda, A., Higashi, Y., Tadanaga, K., & Tatsumisago, M. (2006). Hot-water treatment of sol–gel derived SiO_2–TiO_2 microparticles and application to electrophoretic deposition for thick films. *Journal of Materials Science*, *41*, 8101–8108. DOI: 10.1007/s10853-006-0419-7.

Oikonomou, P., Dedeloudis, C., Stournaras, C. J., & Ftikos, C. (2007). Stabilized tialite–mullite composites with low thermal expansion and high strength for catalytic converters. *Journal of the European Ceramic Society*, *27*, 3475–3482. DOI: 10.1016/j.jeurceramsoc.2006.07.020.

Okada, K., & Otsuka, N. (1986). Characterization of the spinel phase from SiO_2–Al_2O_3 xerogels and the formation process of mullite. *Journal of the American Ceramic Society*, *69*, 652–656. DOI: 10.1111/j.1151-2916.1986.tb07466.x.

Periyat, P., Baiju, K. V., Mukundan, P., Pillai, P. K., & Warrier, K. G. K. (2008). High temperature stable mesoporous anatase TiO_2 photocatalyst achieved by silica addition. *Applied Catalysis A*, *349*, 13–19. DOI: 10.1016/j.apcata.2008.07.022.

Pourbaix, M. (1974). *Atlas of electrochemical equilibria in aqueous solutions*. Oxford, UK: Pergamon.

Richmond, W. R., Jones, R. L., & Fawell, P. D. (1998). The relationship between particle aggregation and rheology in mixed silica–titania suspensions. *Chemical Engineering Journal*, *71*, 67–75. DOI: 10.1016/s1385-8947(98)00105-3.

Schneider, H., & Komarneni, S. (2005). *Mullite*. Weinheim, Germany: Wiley. DOI: 10.1002/3527607358.

Sobhani, M., Ebadzadeh, T., & Rahimipour, M. R. (2014). Formation and densification behavior of reaction sintered

alumina-20 wt. % aluminium titanate nano-composites. *International Journal of Refractory Metals and Hard Materials*, *47*, 49–53. DOI: 10.1016/j.ijrmhm.2014.06.018.

Wellia, D. V., Xu, Q. C., Sk, M. A., Lim, K. H., Lim, T. M., & Tan, T. T. Y. (2011). Experimental and theoretical studies of Fe-doped TiO_2 films prepared by peroxo sol–gel method. *Applied Catalysis A*, *401*, 98–105. DOI: 10.1016/j.apcata.2011.05.003.

Wu, Z. J., Yue, H. F., Li, L. S., Jiang, B. F., Wu, X. R., & Wang, P. (2010). Synthesis and electrochemical properties of multi-doped $LiFePO_4$/C prepared from the steel slag. *Journal of Power Sources*, *195*, 2888–2893. DOI: 10.1016/j.jpowsour.2009.11.058.

Wu, X. R., Wang, H. H., Li, L. S., Lü, H. H., Wu, Z. J., & Shen, X. M. (2013a). Synthesis of cordierite powder from blast furnace slag. *Transactions of the Indian Ceramic Society*, *72*, 197–200. DOI: 10.1080/0371750x.2013.851622.

Wu, X. R., Lü, H. H., Li, L. S., Wang, P., Shen, X. M., Zhu, J. H., Cao, F. B., & Li, M. H. (2013b). China Patent No. 201110101537.3. Beijing, China: China Patent & Trademark Office. http://www.pss-system.gov.cn/sipopublicsearch/search/searchHome-searchIndex.shtml?params=991CFE73D4DF553253D44E119219BF31366856FF4B152226CAE4DB031259396A

Xie, X., Sun, J., Liu, Y., & Jiang, W. (2010). Use of silica sol as a transient phase for fabrication of aluminium titanate–mullite ceramic composite. *Scripta Materialia*, *63*, 641–644. DOI: 10.1016/j.scriptamat.2010.05.038.

Zhou, S. X., Antonietti, M., & Niederberger, M. (2007). Low-temperature synthesis of γ-alumina nanocrystals from aluminum acetylacetonate in nonaqueous media. *Small*, *3*, 763–767. DOI: 10.1002/smll.200700027.